Increase in strength due to suction for two Hong Kong soils

D.Y.F. Ho and D.G. Fredlund

Abstract: The surficial, residual soils of Hong Kong are unsaturated *in situ*, having negative pore-water pressures which contribute to their strength. The major geotechnical problem in Hong Kong is the stability of natural slopes of decomposed granite and decomposed volcanics (rhyolite). For many years, the stability of these extremely steep slopes has been attributed to matric suction (i.e., the negative pore-water pressure in the soil); however, the significance of suction has never been quantified.

The paper presents the results of the measurement of the shear strength parameters of the two mentioned Hong Kong residual soils and quantitatively interprets their significance in the light of the slope stability problem. More specifically, the paper deals with the relationship between soil suction and shear strength for the Hong Kong soils.

The testing program involved multi-stage triaxial tests. This procedure was chosen to eliminate the effect of the variability of residual soils. Seventeen 2 ½ inch diameter, undisturbed samples were tested, including ten decomposed granites and seven decomposed volcanics (rhyolite). During the test, air and water pressures were controlled to maintain constant suction in the soil specimen throughout any stage of the test. With a 5 bar, high air entry disk installed at the bottom of a modified triaxial cell, the axis-translation technique was used to control the matric suction in the specimen.

The unsaturated soil shear strength theory of Fredlund et al. (1978) was used as basis for the interpretation of data.

The paper concludes that the increase in strength due to suction, $(u_a - u_w)$, can be evaluated from a single triaxial test using the multistage procedure. The most convenient form for expressing the increase in shear strength due to suction is as an increase in the cohesion:

$$c = c' + (u_a - u_w)\tan\phi^b$$

where:

c = total cohesion of the soil.

In other words, the suction in an unsaturated soil increases the cohesion of the soil. Accordingly, the shear strength parameters used in a slope stability analysis should be modified to reflect the *in situ* soil suction conditions.

Key words: unsaturated soil, matric suction, cohesion, shear strength, Hong Kong soils, triaxial test, slope stability, axis translation technique.

Introduction

Slope failures are common in Hong Kong. In general, most of the natural slopes in Hong Kong have soils that are desiccated to a considerable depth and the water table is far below ground surface. These steep slopes stand well in dry seasons but collapse when there is continuing precipitation. Traditionally, Janbu's et al. (1956) simplified method and saturated soil shear strength parameters, (i.e., the effective cohesion, c', and the effective friction angle, ϕ'), are used in slope stability analyses.

D.Y.F. Ho. Geotechnical Engineer, Fugro (Hong Kong) Ltd., 105 Asian House, 1 Hennessy Road, Hong Kong.
D.G. Fredlund. Professor, Department of Civil Engineering, University of Saskatchewan, 57 Campus Drive, Saskatoon, SK, S7N 5A9 Canada.

Reproduced with permission from the *Proceedings, ASCE Geotechnical Conference on Engineering and Construction in Tropical and Residual Soils*, Honolulu, Hawaii, 1982. pp. 263–295.

The computed factor of safety often gives values that are less than 1.0, even for stable slopes. In other words, either there is a deficiency in the method of analysis or else there is a deficiency in the procedure used to evaluate the shear strength parameters.

Through a parametric study of various methods of slope stability analyses, Ching (1981) demonstrated that the quantitative difference between factors of safety computed using different methods appears to be of secondary significance for the Hong Kong conditions. However, an increase in the input cohesion parameter in a stability analysis significantly increases the computed factor of safety. Fredlund (1979) suggested that the suction of a soil could be considered as an increase in cohesion. This suggests that soil suction may be a significant factor in the stability of slopes in Hong Kong (Fredlund 1981). In other words, the slopes are stable because of the existence of suction and become unstable if soil suction is negated.

This paper presents the results of the measurement of the shear strength parameters of two commonly found Hong Kong residual soils and interprets their significance in view of the slope stability problem. More specifically, the paper deals with the relationship between soil suction and shear strength for the Hong Kong residual soils.

The shear strength theory for unsaturated soils

Fredlund et al. (1978) proposed a shear strength equation for unsaturated soils which was an extension of the commonly used Mohr-Coulomb equation (Terzaghi 1936) for saturated soils. In the extended form of the Mohr-Coulomb equation, the effect of matric suction, $(u_a - u_w)$, is assumed to yield a linear increase in shear strength. When $(\sigma - u_a)$ and $(u_a - u_w)$ are used as the stress state variables, the proposed unsaturated soil shear strength equation is as follows:

$$[1] \quad \tau = c' + (\sigma - u_a)\tan\phi' + (u_a - u_w)\tan\phi^b$$

The friction angle, ϕ^b, is equal to the slope of the plot of matric suction, $(u_a - u_w)$, versus shear strength, when $(\sigma - u_a)$ is held constant. The form of the equation describes a plane on a three-dimensional plot (Fig. 1). The stress circles corresponding to the failure conditions can be plotted on a three-dimensional diagram with the two stress state variables plotted on the horizontal axes and the shear strength as the ordinate (Fig. 2). Test data can be interpreted by either a mathematical (Fredlund et al. 1978) or a graphical method (Fredlund 1981; Ho 1981). The interpretation of the data is easier to visualize using the graphical method and for this reason will be used throughout this paper.

Using the graphical method, the equation can be visualized as a two-dimensional graph with matric suction contoured as the third variable (Fig. 3*a*). Consequently, the ordinate intercepts of the various matric suction contours (i.e., when $(\sigma - u_a)$ is equal to zero) can be plotted versus matric suction to give the friction angle, ϕ^b (Fig. 3*b*).

There is a smooth transition from Fredlund et al. (1978) unsaturated soil shear strength equation to the conventional shear strength equation for saturated soils (Terzaghi 1936). As saturation is approached, the pore-air pressure, u_a, becomes equal to the pore-water pressure, u_w. At this condition, the proposed equation reverts to the conventional shear strength equation for a saturated soil.

Verification of the shear strength theory for unsaturated soils

The justification for the linear form of the unsaturated soil shear strength equation must be verified by experimental laboratory test data.

Bishop et al. (1960) presented several sets of triaxial test data for unsaturated soils. Two sets of data were from constant water content tests with pore-air and pore-water pressure measurements. The soils tested were compacted shale and a Boulder clay. The data have been reanalysed using the mathematical and graphical methods (Fredlund et al. 1978; Ho 1981). The results are summarized in Table 1.

It can be seen that the correlation coefficients for the ordinate intercepts versus matric suction plots are high (i.e., between 0.97 and 0.98). If the surface describing stress combinations at failure were ideally planar, the ordinate intercepts versus matric suction plot should be a straight line having a correlation coefficient of 1.0.

Satija (1978) initiated an extensive laboratory testing program on statically compacted Dhanauri clay. Four series of constant water content (CW) and consolidated drained (CD) tests were conducted with pore-air and pore-water pressure measurements. The soil was compacted at two densities but with the same initial water contents. Both the constant water content and consolidated drained tests were performed at each of the com-

Fig. 1. Graphical representation of the shear strength equation for unsaturated soils.

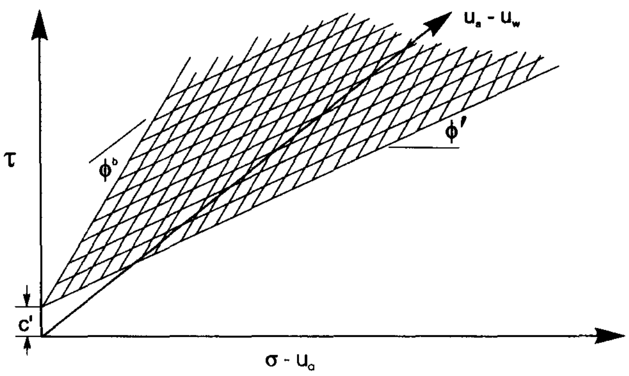

Fig. 2. Three-dimensional failure surface using stress variables $(\sigma - u_a)$ and $(u_a - u_w)$.

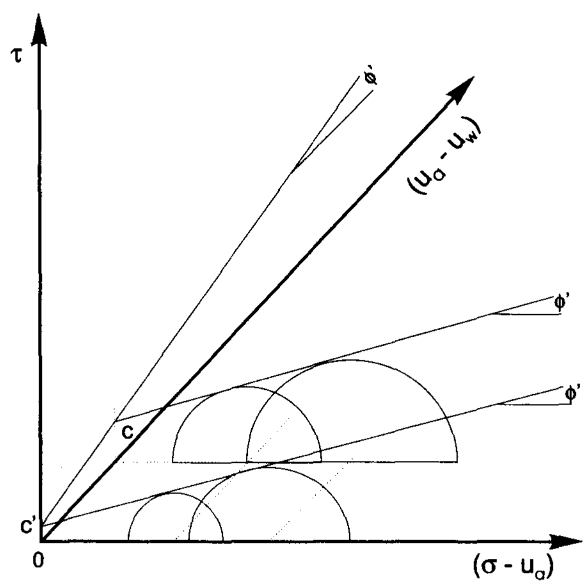

Table 1. Triaxial tests on unsaturated soils (Bishop et al. 1960).

Soil type	c' (kPa)	ϕ' (degrees)	ϕ^b (degrees)	Correlation coefficients*
Compacted shale w = 18.6%	15.8	24.8	18.1	0.970
Boulder clay w = 11.6%	9.6	27.3	21.7	0.974

* Correlation coefficient is for the computation of ϕ^b.

Fig. 3. *a*) Failure surface of an unsaturated soil looking parallel to the $(u_a - u_w)$ axis; *b*) Interpretation of a multi-stage triaxial test to get the angle of friction with respect to matric suction.

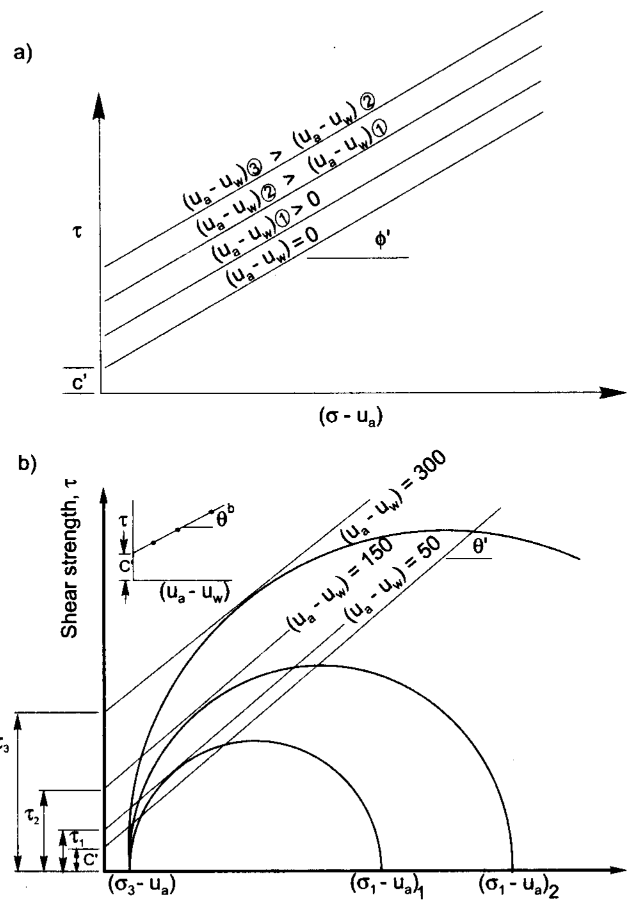

paction conditions. Although the specimens for a particular series of tests were compacted at the same density and water content, they were allowed to equalize to various initial stress states to form an equally spaced grid of tests on a three-dimensional surface. The original data have been reanalysed using the graphical method (Ho 1981). Figure 4*a* shows the failure stress circles for one series of the constant water content tests performed on specimens with a high initial density. The shear strength versus matric suction plot for all the constant water content tests on the high initial density specimens is shown in Fig. 4*b*. The results are summarized in Table 2. The correlation coefficients for all the ordinate intercepts versus matric suction plots are high and reveal no tendency for warping of the failure surface except at low suctions, less than 100 kPa.

Escario (1980) performed direct shear tests with pore pressure controls on compacted Madrid Gray clay. The tests results are shown in Fig. 5*a*. The results have been reanalysed using the graphical method (Ho 1981) and show a ϕ^b angle of 16.1 degrees (Fig. 5*b*). The correlation coefficient is high and there is no indication of warping of the surface describing the stress combinations at failure (Fig. 5*b*).

To date, the published test data demonstrates that the surface describing the stress combination of failure for an unsaturated soil is essentially planar. Although the failure surface could possibly be somewhat curved, especially at low suction, it appears to be sufficiently close to being planar that the unsaturated soil shear strength theory as per Fredlund et al. (1978) is satisfactory for engineering purposes.

Test Program

The two most commonly found Hong Kong residual soils, decomposed granite and rhyolite, were tested in the laboratory program. The mineral compositions of these two residual soils are essentially the same, including quartz, orthoclase, plagioclase and biotite. The main difference between the two soils is their grain size distribution. In general, the decomposed granite has a sand size texture, whereas the decomposed rhyolite has a medium to fine silt size texture. Both residual soils are brittle and highly variable (Lumb 1962, 1965). Undisturbed specimens were obtained from test drilling (using the Fugro sampler) or open cuts (using block samples) at various sites on the Hong Kong island (Table 3).

The test program consisted of triaxial shear tests on both decomposed granite and rhyolite. Seventeen, 2½ inch (6.35 cm) diameter, undisturbed specimens were tested with ten of the specimens being decomposed granite and seven of the specimens being decomposed rhyolite. The test procedure involved the control of the air and water pressures during the entire test rather than their measurements in a closed system (Bishop and Henkel 1962). Since the decomposed granite and rhyolite are comparatively coarse-grained with high coefficients of permeability (Lumb 1965), it is possible to maintain the pore-air and pore-water pressures constant during the application of the deviator stress. The testing procedure is similar to performing a "slow" or drained test on a saturated soil. A 5 bar (i.e., 505 kPa) high air entry disk was sealed into the bottom pedestal of a modified conventional triaxial cell (Fig. 6) in order to separately control

Table 2. Triaxial tests on unsaturated Dhanauri Clay (Satija 1978).

Soil type	c' (kPa)	ϕ' (degrees)	ϕ^b (degrees)	Correlation coefficients*
CD test γ_d = 15.5 kN/m^3 w = 22.2%	37.3	28.5	16.2	0.974
CD test γ_d = 14.5 kN/m^3 w = 22.2%	20.3	29.0	12.6	0.963
CW test γ_d = 15.5 kN/m^3 w = 22.2%	15.5	28.5	22.6	0.992
CW test γ_d = 14.5 kN/m^3 w = 22.2%	11.3	29.0	16.5	0.971

*Refers to the best-fit line for ϕ^b.

Fig. 4. *a*) Mohr failure circles for Dhanauri Clay with high as-compacted density from CW tests, Series 3; *b*) Shear strength versus matric suction for Dhanauri Clay with high as-compacted density from CW tests (from Satija 1978).

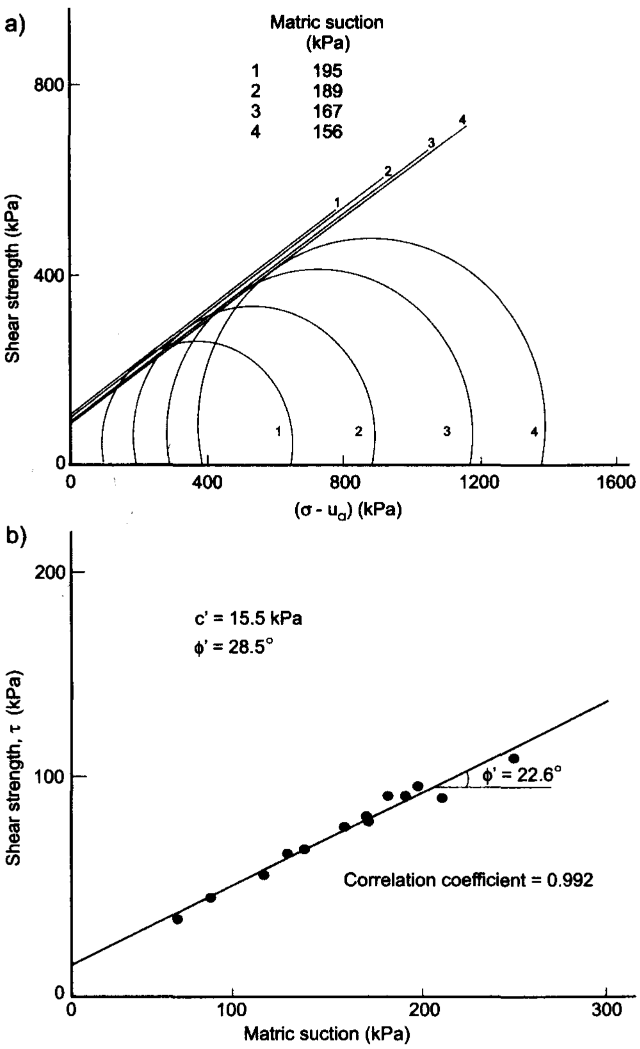

Fig. 5. *a*) Shear strength of Madrid Grey Clay at various suction levels; *b*) Shear strength versus matric suction of Madrid Grey Clay (after Escario 1980).

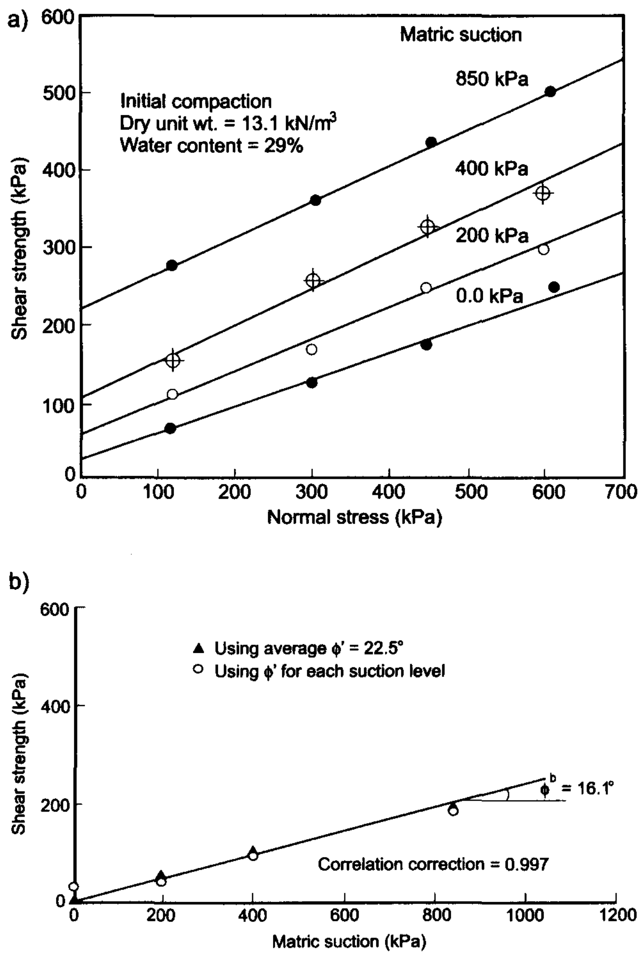

Table 3. Summary of undisturbed specimens used in the test program.

Sample No.	Location	Fugro sampler blowcount	Description of soil sample
5	Hong Kong Hospital and Sanatorium, Happy Valley (depth = 10.15 m)	27	Brownish pink, dense, slightly clayey, sandy silt with some fine gravel. (Completely weathered granite)
6	Hong Kong Hospital and Sanatorium, Happy Valley (depth = 4.65 m)	42	Pink with grey spots, dense to very dense, silt and sand with some fine gravel. (Completely to highly weathered granite)
8	Hong Kong Hospital and Sanatorium, Happy Valley (depth = 14.15 m)	63	Pink with grey spots, dense, sandy silt with some fine gravel. (Completely weathered granite)
10	Hong Kong Hospital and Sanatorium, Happy Valley (depth 4.15 m)	12	Brownish pink, medium dense, slightly clayey, sandy silt with some fine gravel. (Completely weathered granite)
11A 11B 11C 11D	Thorpe Manor Site, Hong Kong (depth = 10.15 m to 10.38 m)	Block Sample	Brownish, medium to fine, slightly clayey, sandy silt. (Decomposed volcanic rock)
12	9 Brewin Path, Hong Kong (depth = 15.0 m to 15.3 m)	65	Light yellowish grey with some white, dense (slightly clayey), silt and fine sand (with some medium and coarse sand). (Completely weathered volcanic rock)
14	9 Brewin Path, Hong Kong (depth = 16.5 m to 16.8 m)	74	Light yellowish grey with some white, dense (slightly clayey), silt and fine sand (with some medium and coarse sand). (Completely weathered volcanic rock)
16	Chun Fai Road, Jardine's Lookout, Hong Kong (depth = 7.5 m to 7.95 m)	87	Yellowish brown, dense silty sand with some fine gravel. (Completely weathered granite)
17	Chun Fai Road, Jardine's Lookout, Hong Kong (depth = 6.0 m to 6.45 m)	23	Orange brown, medium dense sandy silt. (Completely weathered granite)
20	97 Robinson Road, Hong Kong (depth = 22.0 m to 22.3 m)	35	Reddish brown, silty sand with patches of white, plastic, fine clay. (Completely weathered granite)
21	97 Robinson Road, Hong Kong (depth = 14.0 m to 14.3 m)	53	Reddish brown, silty sand with patches of white, plastic, fine clay. (Granitic residual soil)
22	97 Robinson Road, Hong Kong (depth = 4.0 m to 4.3 m)	16	Reddish brown with dark green and white specks, sandy silt with some fine gravel and patches of plastic clay. (Granite residual soil)
23	Chun Fai Road, Jardine's Lookout, Hong Kong (depth =10.5 m to 10.95 m)	49	Yellowish brown with dark green specks, dense sandy silt. (Completely weathered granite)

the pore-air and pore-water pressures. The axis-translation technique (Bocking and Fredlund 1980) was used to impose suctions higher than one atmosphere in the specimen. During the test, the air and water pressures were controlled so as to maintain constant suction in the specimen throughout each stage of the test.

In order to obtain the maximum amount of information from a limited number of tests and eliminate the effect of variability in residual soils, a multi-stage type of test procedures was used (Kenny and Watson 1961; Lumb 1964; Wong 1978). The test procedure was as follows:

(1) The specimen was trimmed for testing. The specimens were 2½ inches (6.35 cm) in diameter and approximately 5½ inches (14.0 cm) long.

(2) The specimen was mounted in the triaxial cell (Fig. 6) and two rubber membranes were placed around the specimen.

(3) O-rings were placed over the membranes on the bottom pedestal and a spacer was placed between the membranes and the loading cap in order that air within the specimen could escape during the saturation process.

(4) To ensure that the suction applied to the specimen for Stage 1 testing was greater than the initial soil suction, the specimens were saturated by allowing the intake of water. De-aired water was added to the specimen through the air pressure line connected to the loading cap.

Fig. 6. Modified triaxial cell for testing unsaturated soils.

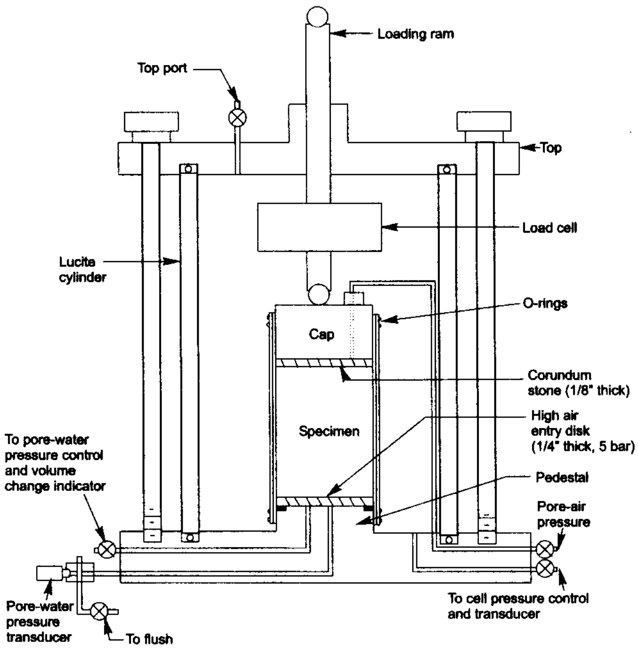

(5) Once-the specimens had fully imbibed water, the top O-rings were placed around the loading cap.
(6) The stress associated with the first stage of testing (i.e., Stage 1) were applied and the specimen was allowed to consolidate. A typical set of stresses for Stage 1, 2 and 3 is as follows:

Stage No.	σ_a (kPa)	u_a (kPa)	u_w (kPa)
1	250	100	50
2	350	200	50
3	500	350	50

The associated stress state variables are:

Stage No.	$(\sigma_3 - u_a)$ (kPa)	$(u_a - u_w)$ (kPa)
1	150	50
2	150	150
3	150	300

(7) After consolidation was complete, the stresses were maintained while the specimen was loaded at a constant strain rate. A typical loading rate was 0.001 percent strain per minute (Ho 1981).
(8) Two kinds of loading procedure (i.e., the cyclic and sustained loading) were used. Once the deviator stress reached a peak value, the applied vertical load was either released (i.e., cyclic loading) or sustained (i.e., sustained loading), (Fig. 7*a* and 7*b*), (Ho 1981).

Fig. 7. *a*) Ideal stress versus strain curves for a multi-stage test using the cyclic loading procedure; *b*) Ideal stress versus strain curves for a multi-stage test using the saturated loading procedure.

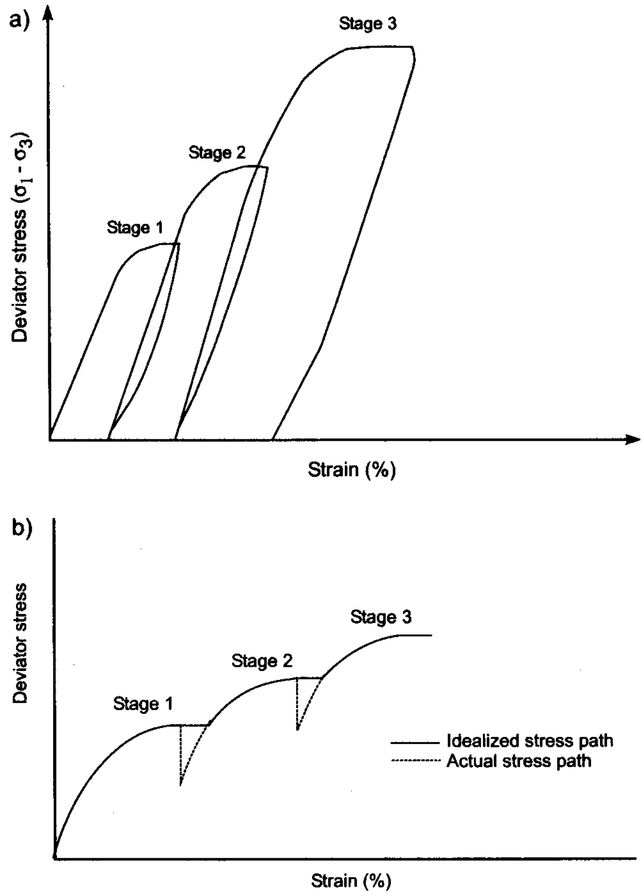

(9) A new set of stresses for Stage 2 was applied to the specimen, consolidation was again allowed and the loading process was repeated as before.
(10) The above procedure was further applied to Stage 3.

Presentation of Data

Stress measurements made in the multi-stage triaxial tests are summarized in Table 4. The stress σ_1 was computed from the measured load and calculated cross-sectional area. Deviator stress versus strain plots for six decomposed granite and six decomposed rhyolite specimens are presented in Figs. 8*a* to 13*b*.

In general, the deviator stress of most of the specimens dropped off significantly immediately after peaking in Stage 3. The specimens seemed to show signs of structural breakdown or collapse in the third stage of loading. The amount of strength "drop-off" in Stage 3 appeared to be related to the amount of accumulated strain. Problems associated with excessive deformation in multi-stage triaxial tests have been noted by other researchers (Kenny

Table 4. Stress measurements made in the multi-stage triaxial tests.

Sample No.	Stage No	σ_3 (kPa)	u_a (kPa)	u_w (kPa)	σ_1 (kPa)	$(\sigma_3 - u_a)$ (kPa)	$(\sigma_1 - u_a)$ (kPa)	$\frac{(\sigma_1 - \sigma_3)}{2}$ (kPa)	$(u_a - u_w)$ (kPa)	$\frac{(\sigma_1 + \sigma_3)}{2} - u_a$ (kPa)
5	1	206.9	68.9	68.95	613.7	137.9	544.7	203.4	0.0	341.3
	2	448.2	310.3	68.95	1102.0	137.9	791.2	326.7	214.3	464.6
	3	689.5	551.6	68.95	1496.0	137.9	944.6	403.4	482.2	541.3
6	1	241.3	103.4	68.95	794.8	137.9	691.4	276.8	34.5	414.7
	2	344.8	206.9	68.95	1019.0	137.9	811.8	336.9	137.9	474.9
	3	517.1	310.3	68.95	1636.0	137.9	1325.0	599.3	241.3	766.2
8	1	241.3	103.4	68.95	976.9	137.9	873.5	367.8	34.5	505.7
	2	344.8	206.9	68.95	1179.0	137.9	972.1	417.1	137.9	554.9
	3	517.1	310.3	68.95	1639.0	137.9	1328.0	560.8	241.3	767.6
10	1	241.3	103.4	68.95	725.4	137.9	621.9	242.0	34.5	379.9
	2	344.8	206.9	68.95	952.3	137.9	745.5	303.8	137.9	441.2
	3	448.2	310.3	68.95	1143.0	137.9	833.1	347.6	241.3	485.5
11A	1	241.3	103.4	68.95	747.8	137.9	644.4	253.3	34.5	391.2
	2	344.8	206.9	68.95	946.9	137.9	740.0	301.0	137.9	438.9
	3	448.2	310.3	68.95	1120.0	137.9	809.4	335.8	241.3	473.7
11B	1	241.3	103.4	68.95	875.0	137.9	771.6	316.9	34.5	454.8
	2	344.8	206.9	68.95	1083.0	137.9	875.6	368.9	137.9	506.8
	3	448.2	310.3	68.95	1221.0	137.9	910.9	386.5	241.3	524.4
11C	1	241.3	103.4	68.95	790.9	137.9	687.5	274.8	34.5	412.7
	2	344.8	206.9	68.95	1020.0	137.9	813.5	337.8	137.9	475.7
	3	448.2	310.3	68.95	1210.0	137.9	899.4	380.8	241.3	518.7
11D	1	241.3	103.4	68.95	855.7	137.9	752.3	307.2	34.5	445.1
	2	344.8	206.9	68.95	1080.0	137.9	873.3	367.7	137.9	505.6
	3	448.2	310.3	68.95	1298.0	137.9	987.9	425.0	241.3	562.9
12	1	137.9	103.4	68.95	288.9	34.48	185.5	75.5	34.5	109.9
	2	241.3	206.9	68.95	530.2	34.48	323.4	144.5	137.9	178.9
	3	344.8	310.3	68.95	680.8	34.48	370.5	168.0	241.3	202.5
14	1	137.9	103.4	68.95	313.3	34.48	209.9	87.7	34.5	122.2
	2	241.3	206.9	68.95	542.6	34.48	335.8	150.6	137.9	185.1
	3	344.8	310.3	68.95	681.5	34.48	371.2	168.4	241.3	202.8
15	1	137.9	103.4	68.95	292.4	34.48	188.9	77.3	34.5	111.7
	2	241.3	206.9	68.95	607.1	34.48	400.3	182.9	137.9	217.4
	3	344.8	310.3	68.95	754.8	34.48	444.5	205.0	241.3	239.5
16	1	137.9	103.4	68.95	694.0	34.48	590.6	278.1	34.5	312.5
	2	172.4	206.9	68.95	753.8	34.48	615.9	290.7	137.9	325.2
	3	241.3	310.3	68.95	786.3	34.48	579.5	272.5	241.3	306.9
17	1	137.9	103.4	68.95	449.9	34.48	346.5	156.0	34.5	190.5
	2	172.4	206.9	68.95	494.4	34.48	356.5	161.0	137.9	195.5
	3	241.3	310.3	68.95	543.3	34.48	335.5	151.0	241.3	185.5
20	1	137.9	103.4	68.95	426.2	34.48	322.8	144.2	34.5	178.6
	2	172.4	206.9	68.95	507.8	34.48	369.9	167.7	137.9	202.2
	3	241.3	310.3	68.95	620.1	34.48	413.3	189.4	241.3	223.9
21	1	137.9	103.4	68.95	437.9	34.48	334.5	150.0	34.5	184.5
	2	172.4	206.9	68.95	492.4	34.48	354.5	160.0	137.9	184.5
	3	241.3	310.3	68.95	626.4	34.48	419.5	192.6	241.3	227.0
22	1	137.9	103.4	68.95	343.9	34.48	240.5	103.0	34.5	137.5
	2	172.4	206.9	68.95	441.1	34.48	303.2	134.4	137.9	168.8
	3	241.3	310.3	68.95	608.0	34.48	401.2	183.2	241.3	217.8
23	1	137.9	103.4	68.95	747.4	34.48	643.9	304.8	34.5	339.2
	2	172.4	206.9	68.95	805.6	34.48	667.7	316.6	137.9	351.1
	3	241.3	310.3	68.95	905.8	34.48	698.0	332.3	241.3	366.7

Fig. 8. *a*) Stress versus strain curves for decomposed granite (Sample No. 5); *b*) Stress versus strain curves for decomposed granite (Sample No. 10).

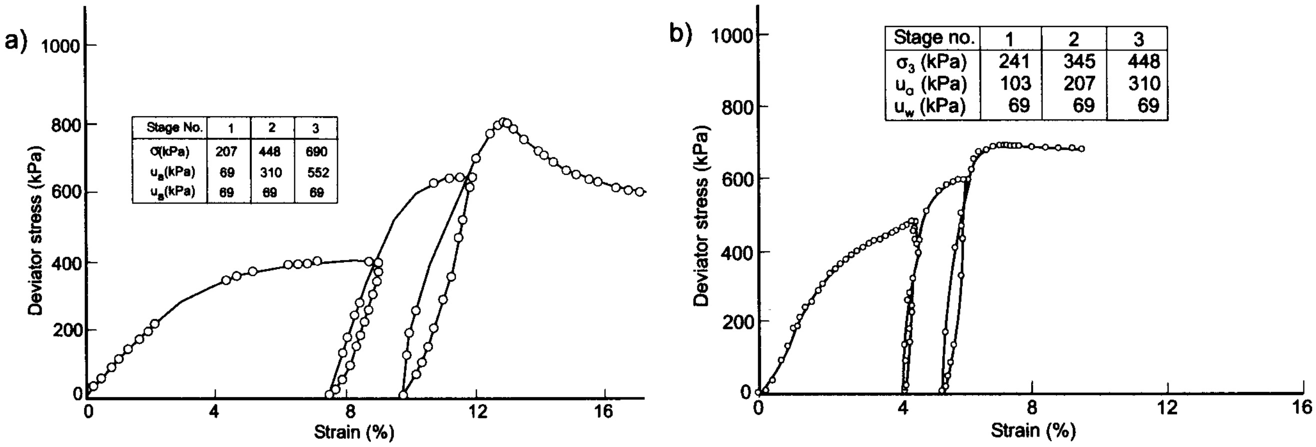

Fig. 9. *a*) Stress versus strain curves for decomposed granite (Sample No. 16); *b*) Stress versus strain curves for decomposed granite (Sample No. 20).

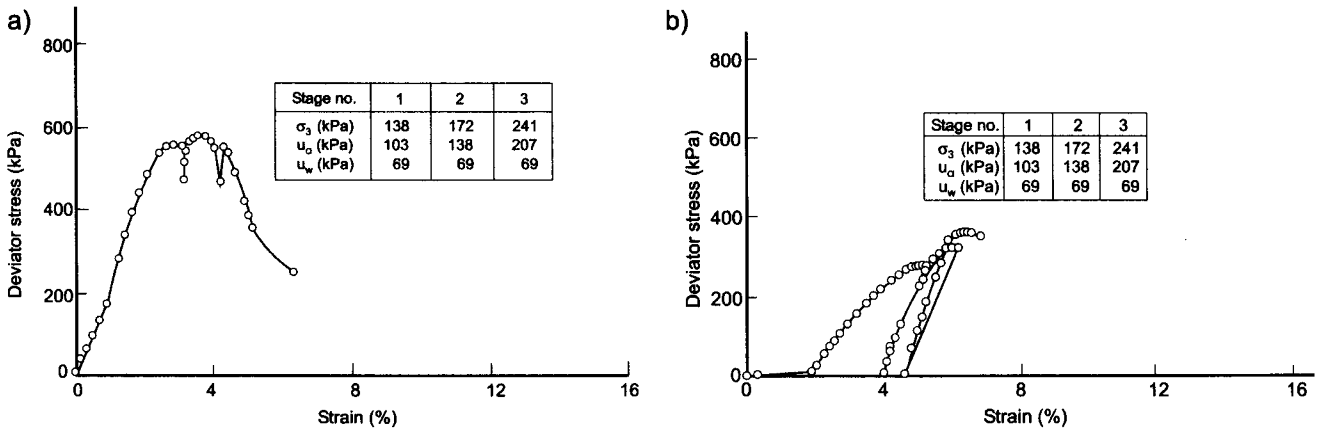

Fig. 10. *a*) Stress versus strain curves for decomposed granite (Sample No. 21); *b*) Stress versus strain curves for decomposed granite (Sample No. 22).

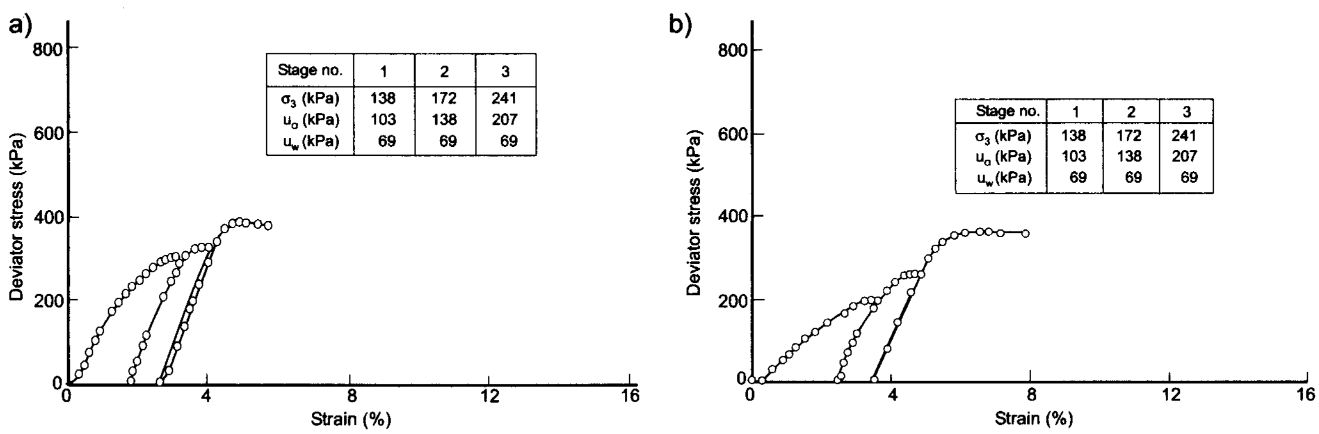

and Watson 1961; Wong 1978). It is suggested that the specimen should not be deformed excessively during the earlier stage of loading. When the specimen is overstrained, the specimen will tend to develop a shear failure plane and undergo a strength decrease. The measured strength will then tend towards the ultimate shear strength. Therefore strain accumulation can be a problem to multi-stage testing.

Fig. 11. *a*) Stress versus strain curves for decomposed rheolite (Sample No. 11A); *b*) Stress versus strain curves for decomposed rheolite (Sample No. 11B).

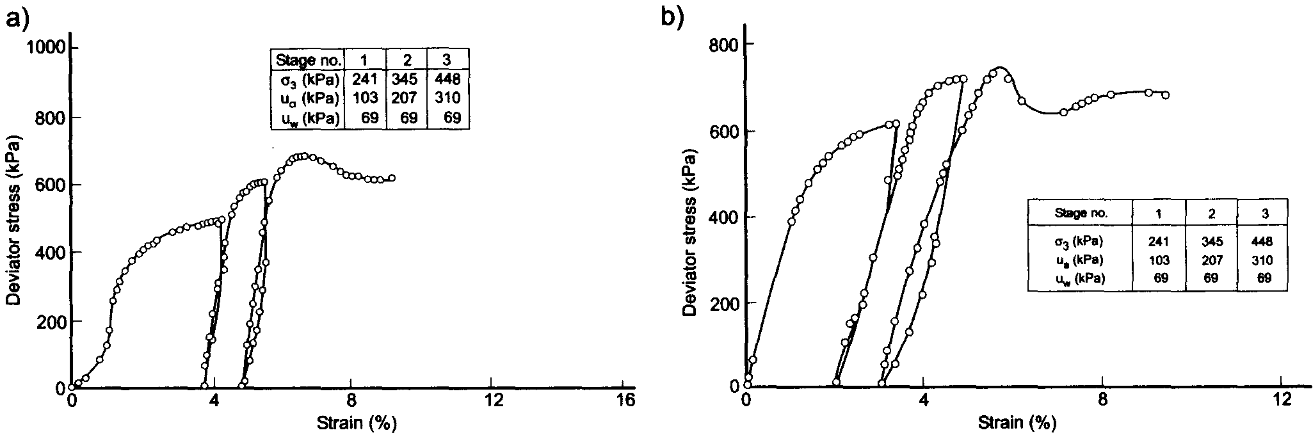

Fig. 12. *a*) Stress versus strain curves for decomposed rheolite (Sample No. 11C); *b*) Stress versus strain curves for decomposed rheolite (Sample No. 11D).

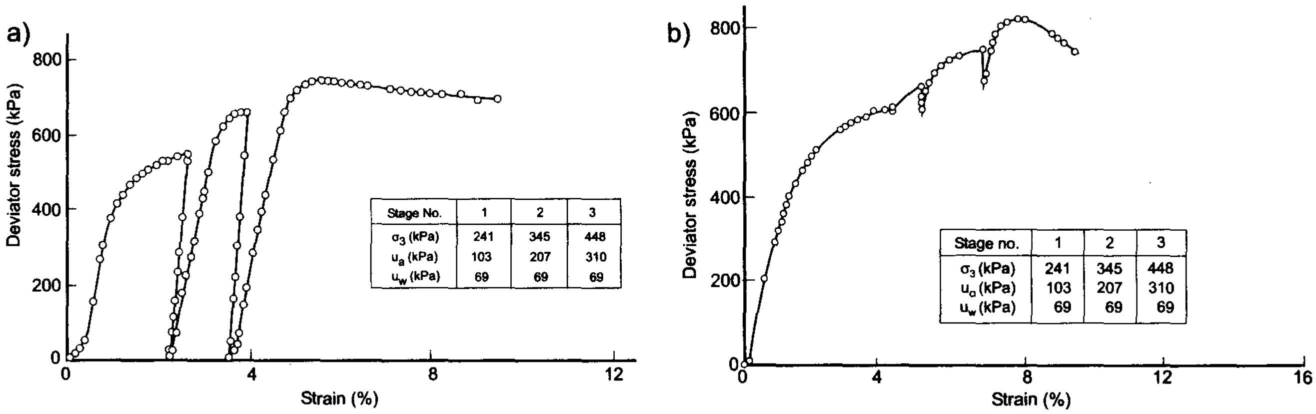

Fig. 13. *a*) Stress versus strain curves for decomposed rheolite (Sample No. 12); *b*) Stress versus strain curves for decomposed rheolite (Sample No. 14).

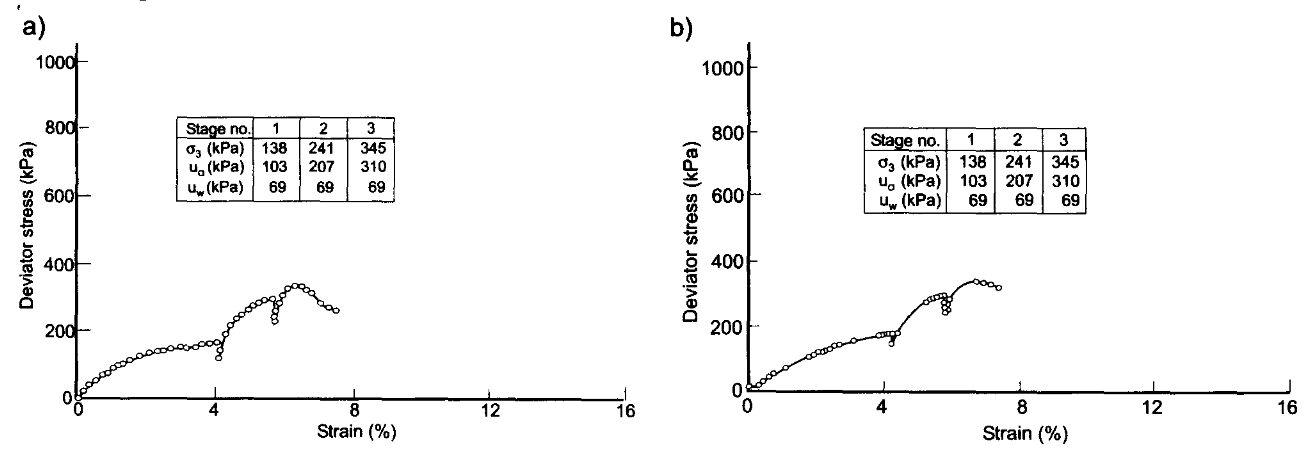

The cyclic loading procedure is preferable to the sustained loading procedure in reducing accumulated strain in the specimen. The advantages associated with releasing the applied deviator stress between stages are as follows. First, it prevents further straining of the soil structure under sustained loading. Second, part of the accumulated strain can be restored through elastic recovery (Figs. 8*a*, 8*b* and 9*b* to 12*a*). If the load on the speci-

Table 5a. Summary of the unsaturated shear strength parameters for the decomposed granite samples (by the graphical method).

Sample No.	5	6	8	10	16	17	20	21	22	23
ϕ^b (degrees)	12.4	27.4	14.6	16.2	11.5	4.2	12.5	12.6	22.5	8.0

* Outlier (ignored).
** ϕ' (input) = 33.4° (Fugro data)***; c' (input) = 28.9 kPa (Fugro data)***.
***Fugro (Hong Kong) Limited, Unpublished Site Investigation Report for 14–23 Fung Fai Terrace, Hong Kong, 1979.

Table 5b. Summary of the unsaturated shear strength parameters for the decomposed rhyolite samples (by the graphical method).

Sample No.	11A	11B	11C	11D	12	14	15
ϕ^b (degrees)	11.7	10.9	15.9	15.4	13.3	11.7	17.7

* ϕ' (input) = 35.3° (Fugro data)**; c' (input) = 7.35 kPa (Fugro data)**.
** Fugro(Hong Kong) Limited, Unpublished Site Investigation Report for 9 Brewin Path, Hong Kong, 1979.

men is sustained between stages, the specimen may continue to deform by creep (Fig. 9*a*).

Analysis of Results

The test data were analyzed in accordance with the unsaturated soil shear strength theory to establish the relationship between soil suction and shear strength. The unsaturated soil shear strength parameter, ϕ^b, is used as a means to quantify the effect of soil suction to the shear strength of the two Hong Kong residual soils. The graphical method was used to analyse the data. Plots showing the stress conditions of failure for each stage, as well as the interpretation of data for twelve of the specimens tested are shown in Figs. 14*a* to 19*b*. The relationship between matric suction and shear strength for each specimen is also shown on each figure. The results of all seventeen multi-stage triaxial tests are summarized in Tables 5*a* and 5*b*.

The average angle of friction with respect to matric suction, ϕ^b, is 15.3 degrees with a range from 8.0 degrees to 27.4 degrees and a standard deviation of ±5.7 degrees for the decomposed granite. The average angle of friction with respect to matric suction is 13.8 degrees with a range from 10.9 degrees to 17.7 degrees and standard deviation of ±2.4 degrees for the decomposed rhyolite. Much of the dispersion associated with the measured angles of friction, ϕ^b, are related to the learning associated with the new testing procedure. It is also recognized that some of the specimens were subjected to excessive strains in the last stage of testing.

As a multi-stage test progresses, the soil structure of a specimen is disturbed to some degree. The change in strength with increasing strain is demonstrated by observing the change in ϕ^b angle from Stage 1 to Stage 3. From the matric suction $(u_a - u_w)$, versus shear strength plots, the angles of friction, ϕ^b, based on the Stage 2 and 3 data are summarized in Tables 6*a* and 6*b*.

Table 6*a* shows that there was an average ϕ^b reduction of 2.1 degrees for the decomposed granite. The comparable ϕ^b reduction for the decomposed rhyolite was 7.5 degrees. It is evident that there is a significant strength reduction in a specimen during the multi-stage shear test. Based on the limited test data, it appears the rhyolite is more susceptible to the structural disturbance caused by multi-stage testing than the decomposed granite.

Conclusion

There is a definite relation between soil suction and shear strength for the Hong Kong residual soils. An increase in soil suction increases strength in accordance with the ϕ^b angle of friction. The proposed multistage triaxial testing procedure can be used to evaluate the increase in strength due to soil suction from a single test.

The average angle of friction with respect to matric suction, ϕ^b, is found to be 15.3 degrees with a standard deviation of ±5.7 degrees for the decomposed granite. The average angle of friction with respect to matric suction, ϕ^b, is found to be 13.8 degrees with a standard deviation of ±2.4 degrees for the decomposed rhyolite. When only the Stage 1 and 2 test results are considered, the average ϕ^b angle is 15.5 degrees with a standard deviation of ±5.3 degrees for the decomposed granite. Similarly, the average ϕ^b angle is 17.6 degrees with a standard deviation of ±4.9 degrees for the decomposed rhyolite.

In order to assess the *in situ* conditions of the Hong Kong residual soils, the effect of soil suction should be included in the evaluation of the shear strength. The effect of soil suction is of particular interest in the analysis of slope stability problems. The matric suction term in the shear strength equation for an unsaturated soil can be considered as contributing to the cohesion of the soil.

$$c = c' + (u_a - u_w) \tan \phi^b$$

where:

c = total or apparent cohesion of the soil.

In other words, the suction in an unsaturated soil increases the cohesion of an unsaturated soil. In this case, conventional soil shear strength concepts can be applied to practical slope stability problems.

Fig. 14. *a*) Graphical analysis for decomposed granite (Sample No. 5); *b*) Graphical analysis for decomposed granite (Sample No. 10).

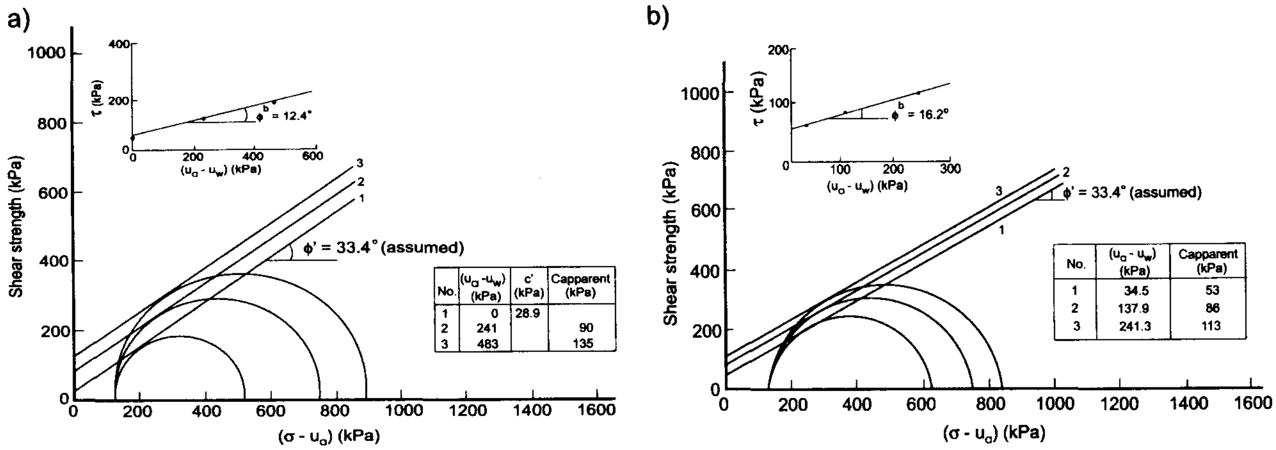

Fig. 15. *a*) Graphical analysis for decomposed granite (Sample No. 16); *b*) Graphical analysis for decomposed granite (Sample No. 20).

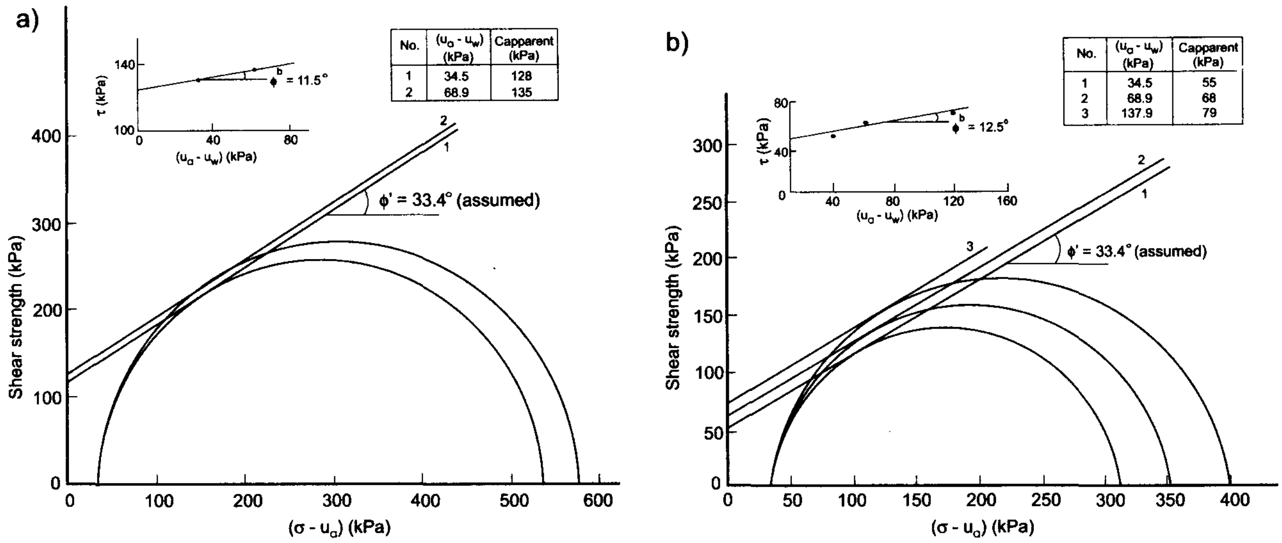

Fig. 16. *a*) Graphical analysis for decomposed granite (Sample No. 21); *b*) Graphical analysis for decomposed granite (Sample No. 22).

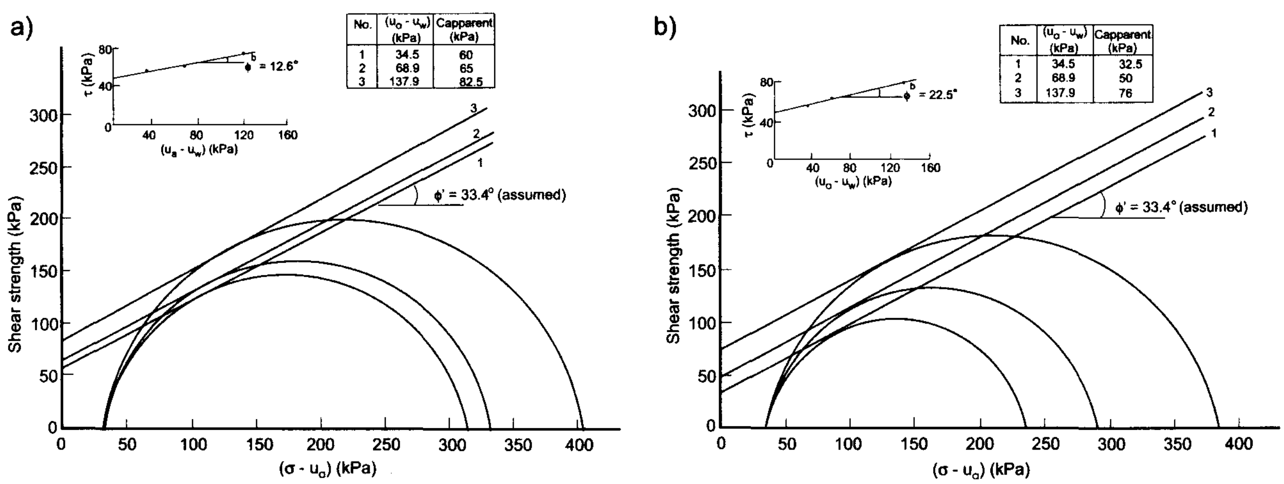

Fig. 17. *a*) Graphical analysis for decomposed rhyolite (Sample No. 11A); *b*) Graphical analysis for decomposed rhyolite (Sample No. 11B).

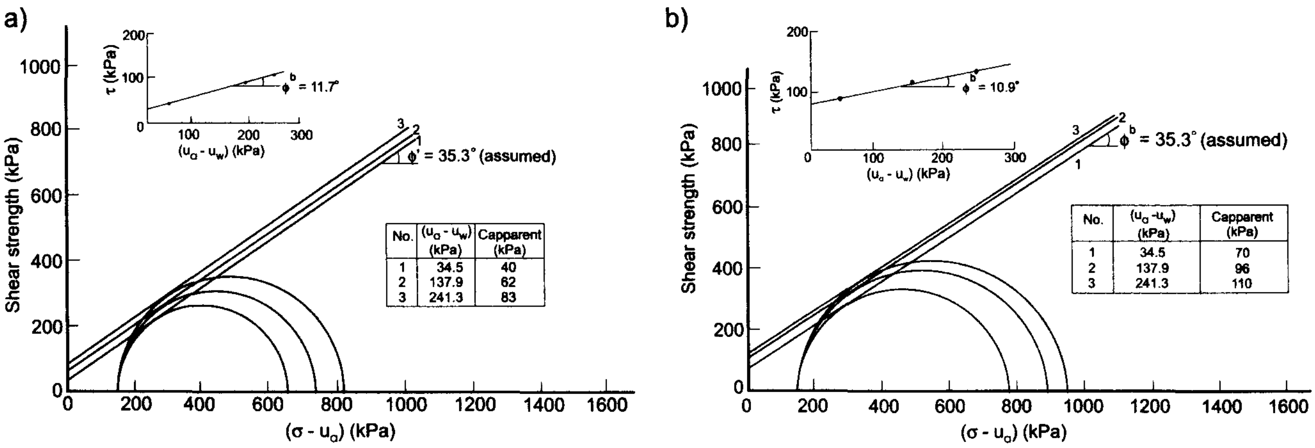

Fig. 18. *a*) Graphical analysis for decomposed rhyolite (Sample No. 11C); *b*) Graphical analysis for decomposed rhyolite (Sample No. 11D).

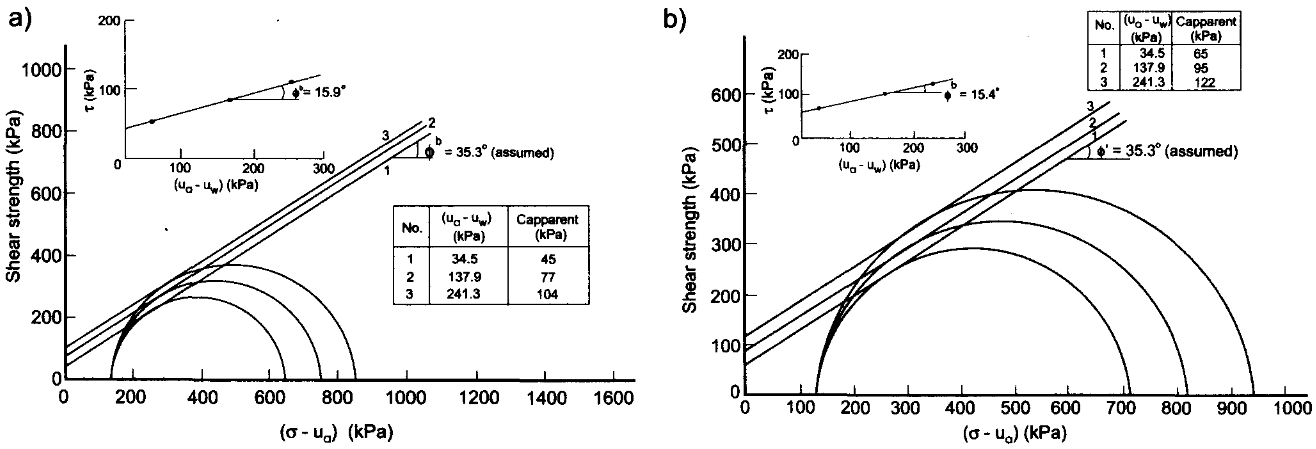

Fig. 19. *a*) Graphical analysis for decomposed rhyolite (Sample No. 12); *b*) Graphical analysis for decomposed rhyolite (Sample No. 14).

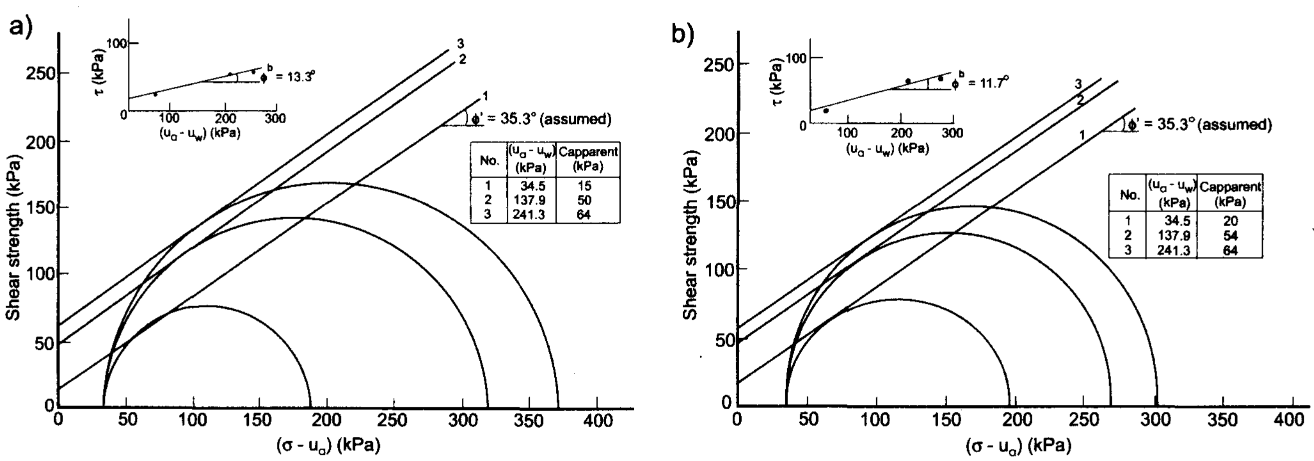

Table 6a. Comparison between ϕ^b values obtained using Stage 1 and 2 and Stage 2 and 3 data (for decomposed granite).

Sample No.	5	6	8	10	16	17	20	21	22	23	Ave.
$\phi^b_{1,2}$ (degrees)	15.0	15.5	13.0	18.5	11.5	4.5*	20.5	8.0	26.5	11.0	15.5 ±5.3**
$\phi^b_{2,3}$ (degrees)	10.0	37.0*	16.5	15.5	—	—	9.5	14.5	21.0	7.0	13.4 ±4.5**

* Outlier (ignored).
** Standard deviation.

Table 6b. Comparison between ϕ^b values obtained using Stage 1 and 2 and Stage 2 and 3 data (for decomposed rhyolite).

Sample No.	11A	11B	11C	11D	12	14	15	Ave.
$\phi^b_{1,2}$ (degrees)	11.0	14.0	18.0	15.5	18.5	18.0	28.0	17.6 ±4.9*
$\phi^b_{2,3}$ (degrees)	12.0	8.0	14.0	15.5	8.5	6.0	7.0	10.1 ±3.4

** Standard deviation.

Acknowledgements

The authors wish to thank the Fugro (Hong Kong) Ltd. for funding the described research work. The establishment of a research scholarship at the University of Saskatchewan has provided opportunity to be involved in a most interesting and challenging problem.

References

Bishop, A.W., Alpan, I., Blight, G. E. and Donald, I. B. 1960. Factors controlling the strength of partly saturated cohesive soils. Proceedings, ASCE Research Conference on Shear Strength of Cohesive Soils, Boulder, Colorado, U.S.A., pp. 503–532.

Bishop, A. W. and Henkel, D. J. 1962. The measurement of soil properties in the triaxial test. Second edition, Edward Arnold Ltd., London, England, 1962.

Bocking, K.A., and Fredlund, D.G. 1980. Limitations of the axis-translation technique. Proceedings, 4th International Conference on Expansive Soils, ASCE, Denver, Colorado, U.S.A., pp. 117–135.

Ching, R. 1981. A theoretical examination and practical applications of the limit equilibrium methods to slope stability problems. M.Sc. thesis, University of Saskatchewan, Saskatoon, SK, Canada.

Escario, V. 1980. Suction controlled penetration and shear tests. Proceedings, 4th International Conference on Expansive Soils, ASCE, Denver, Colorado, U.S.A., Vol. 2, pp. 781–797.

Fredlund, D. G. 1979. Second Canadian geotechnical colloquium: Appropriate concepts and technology for unsaturated soils. Canadian Geotechnical Journal, **16**(1): 121–139.

Fredlund, D. G. 1981. The shear strength of unsaturated soils and its relationship to slope stability problems in Hong Kong. The Hong Kong Engineer, Journal of the Hong Kong Institution of Engineers, **9**(4): 37–45.

Fredlund, D.G., Morgenstern, N.R., and Widger, A. 1978. Shear strength of unsaturated soils. Canadian Geotechnical Journal, **15**(3): 313–321.

Ho, D.Y.F. 1981. The shear strength of unsaturated Hong Kong soils. M.Sc. thesis, University of Saskatchewan, Saskatoon, SK, Canada.

Janubu, N., Bjerrum, L., and Kjaernsli, B. 1956. Stabilitetsberegning for fyllinger skjaeringer og naturlige skraninger. Norwegian Geotechnical Publication No. 16, Oslo, Norway.

Kenney, T.C., and Watson, G.H. 1961. Multi-stage triaxial test for determining c' and ϕ' of saturated soils. Proceedings, 5th International Conference on Soil Mechanics and Foundation Engineering, Paris, France, Vol. 1, pp. 191–195.

Lumb, P. 1962. General nature of the soils of Hong Kong. Symposium on Hong Kong Soils, pp. 19–32.

Lumb, P. 1964. Multi-stage triaxial test on undisturbed soils. Civil Engineering and Public Works Review, **59**: 591–595.

Lumb, P. 1965. The residual soils of Hong Kong. Géotechnique, **15**: 180–194.

Satija, D.J. 1978. Shear behaviour of partially saturated soils. Ph.D. thesis, Indian Institute of Technology, New Delhi, India.

Terzaghi, K. 1936. The shearing resistance of saturated soils. Proceedings, 1st International Conference on Soil Mechanics and Foundation Engineering, Cambridge, MA, Vol. 1, pp. 54–56.

Wong, H.Y. 1978. Soil strength parameter determination. The Hong Kong Engineer, Journal of the Hong Kong Institution of Engineers, March, pp. 33–39.

Appendix

The following symbols are used in this paper:

c = total or apparent cohesion
c' = effective cohesion
u_a = pore-air pressure
u_w = pore-water pressure
$(u_a - u_w)$ = matric suction
w = water content of the soil
τ = shear strength
γ_d = dry unit weight
σ = total stress
σ_1 = total major principal stress
σ_3 = total minor principal stress (i.e., total confining stress)
ϕ' = effective friction angle
ϕ^b = friction angle with respect to changes in $(u_a - u_w)$ when $(\sigma - u_a)$ is held constant
$\phi^b_{1,2}$ = angle of friction, ϕ^b, based on the Stage 1 and 2 data
$\phi^b_{2,3}$ = angle of friction, ϕ^b, based on the Stage 2 and 3 data